Fish Population and Behavior Revealed by Instantaneous Continental Shelf-Scale Imaging

Author(s): Nicholas C. Makris, Purnima Ratilal, Deanelle T. Symonds, Srimvasan Jagannathan, Sunwoong Lee and Redwood W. Nero

REFERENCES
Linked references are available on JSTOR for this article:
https://www.jstor.org/stable/3843512?seq=1&cid=pdf-reference#references_tab_contents
You may need to log in to JSTOR to access the linked references.

Fish Population and Behavior Revealed by Instantaneous Continental Shelf–Scale Imaging

Nicholas C. Makris,[1]* Purnima Ratilal,[2] Deanelle T. Symonds,[1] Srinivasan Jagannathan,[1] Sunwoong Lee,[1] Redwood W. Nero[3]

Until now, continental shelf environments have been monitored with highly localized line-transect methods from slow-moving research vessels. These methods significantly undersample fish populations in time and space, leaving an incomplete and ambiguous record of abundance and behavior. We show that fish populations in continental shelf environments can be instantaneously imaged over thousands of square kilometers and continuously monitored by a remote sensing technique in which the ocean acts as an acoustic waveguide. The technique has revealed the instantaneous horizontal structural characteristics and volatile short-term behavior of very large fish shoals, containing tens of millions of fish and stretching for many kilometers.

There is substantial evidence that fish populations are rapidly declining worldwide (1, 2), yet with conventional seagoing survey methods (3–7) it is difficult to accurately enumerate fish populations (6, 8, 9) and nearly impossible to study the behavioral dynamics of very large social groups or shoals of fish (10), including the impacts of population decline (11, 12). This is because conventional methods rely on highly localized measurements made from slow-moving research vessels, which typically survey along widely spaced line transects to cover the vast areas that fish inhabit, and so greatly undersample the environment in time and space, leaving highly ambiguous records. We assessed fish populations with a remote sensing technology involving ocean acoustic waveguide propagation that surveys at an areal rate that is roughly one million times greater than that of conventional fish-finding methods. The waveguide technology makes it possible to continuously monitor fish population dynamics, behavior, and abundance, with minute-to-minute updates over thousands of square kilometers, producing records without aliasing (13, 14) in time and space.

With the waveguide remote-sensing technology, we observed (i) instantaneous hori-
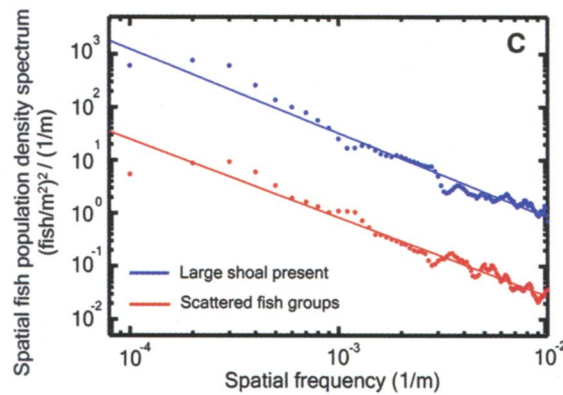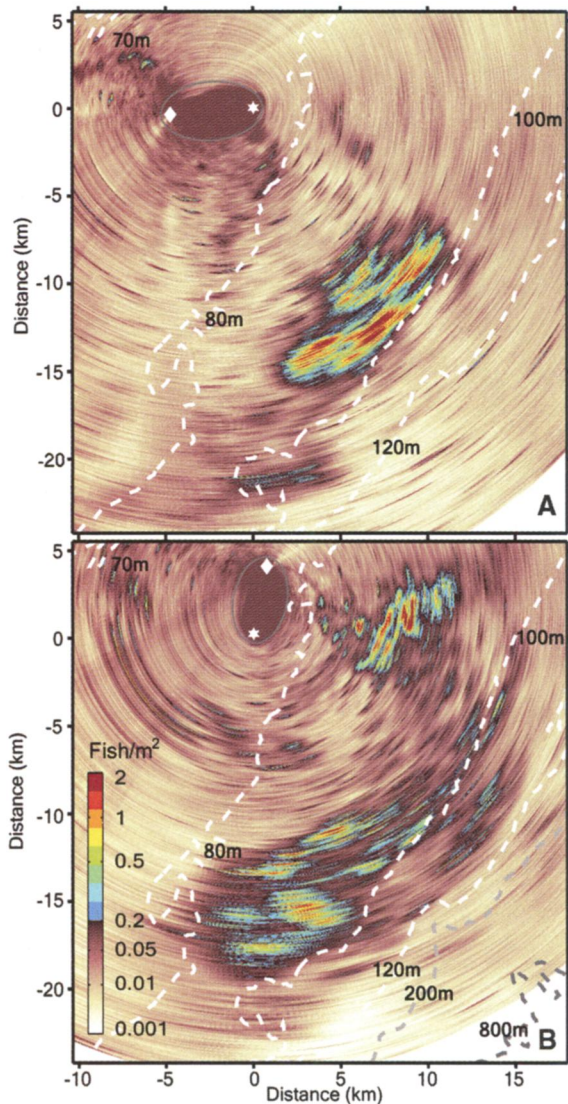
Fig. 1. Two instantaneous areal density images of fish shoals near the continental shelf edge obtained by ocean acoustic waveguide remote sensing (OAWRS) at (A) 09:32 EDT, 14 May 2003, and (B) 08:38 EDT, 15 May 2003, each acquired within 40 s. v_A is shown in color. The moored source (the white star) is the coordinate origin in all figures at 39.0563°N, 73.0365°W. The towed horizontal receiving array (the white diamond) has 2.6° azimuthal resolution at array broadside. The range resolution is 30 m after averaging (14). The forward propagation of sound masks imaging inside the gray ellipse surrounding the source and receiver. The positive vertical axis points north. Depth contours are indicated by dashed lines. In (A) and (B), the continental shelf edge begins at roughly the 100-m contour. (C) Spatial frequency spectra, based on scores of instantaneous OAWRS images of v_A, for cases where a large shoal is present and only small scattered fish groups are present. A consistent spectral power law of spatial frequency to the −1.5 is observed.

zontal structural characteristics, (ii) temporal evolution, and (iii) the propagation of information in very large fish shoals, containing tens of millions of fish and extending for many kilometers. All of these observations were made from distances that were typically greater than 10 km from the shoal boundaries and with sound that was at least three orders of magnitude less intense than conventional fish-finding sonar. This is possible because underwater acoustic remote sensing in the ocean (14–19) relies on the capacity of the continental shelf environment to behave as an acoustic waveguide, in which sound propagates over long ranges via trapped modes that suffer only cylindrical spreading loss rather than the spherical loss suffered in conventional fish-finding sonar technologies (7). The conventional approach employs only waterborne propagation paths that are restricted to much shorter ranges, on the order of the local water depth, and much higher frequencies, where attenuation is much greater (14).
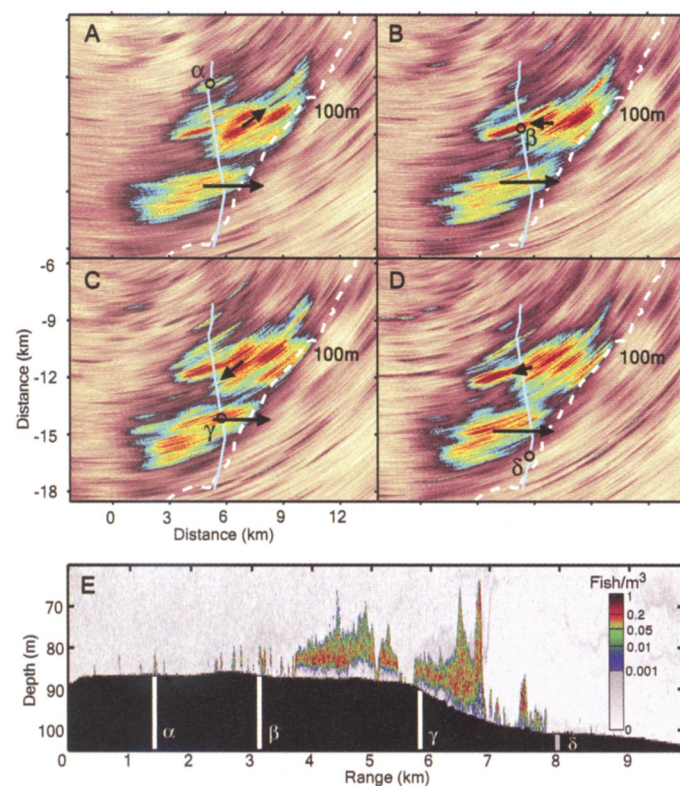
Typical realizations of the instantaneous horizontal structure of very large fish shoals, comprising perhaps the largest massing of animals ever instantaneously imaged in nature, are shown in Fig. 1, A and B. The images are from data acquired during our May 2003 experiment (14) near the edge of the continental shelf 200 km south of Long Island, New York, USA. We found population centers of various size, interconnected by a network of "fish bridges" at various scales. These made the shoal shown in Fig. 1A a contiguous entity that stretched for over 10 km. A similar situation is seen in the very large southern and smaller northern shoal of Fig. 1B. All shoals exhibit large internal vacuoles and hourglass patterns previously observed only in fish groups that were many orders of magnitude smaller in area (9, 10). The shoals are often very sharply bounded on the seaward side by a specific bathymetric contour of the continental shelf edge, as in Fig. 1A. This geophysical boundary apparently organizes the shoal horizontally as a social entity and may also be a navigational landmark for distant migrations (20, 21). Although we found all large shoals between roughly the 80- to 100-m bathymetric contour, fish assemblages changed dramatically over time in any given region, as shown in Fig. 1 from one morning (Fig. 1A) to the next (Fig. 1B). The overall back-

ground population, for example, increases significantly from Fig. 1A to 1B, with a dense distribution of very small groups of fish appearing between the very large southern shoal and the smaller northern one. Under some circumstances, these may provide the building blocks for the fish bridges that bind a shoal together. Annual trawl surveys conducted earlier in the season and historically (14, 22), as well as our visual and behavioral observations at sea, indicate that Atlantic herring, scup, hake, and black sea bass are likely species candidates in the large shoals.

The instantaneous horizontal spatial distribution of fish over wide areas follows a fractal or power-law spectral process, as quantitatively shown in Fig. 1C. Instantaneous structural similarity then exists at all scales observed, from tens of meters to tens of kilometers, and suggests that similar underlying behavioral mechanisms may be responsible for structures at all scales. This supports the qualitative argument for a fractal process in (9) but not the disjoint clustering of population centers that is perhaps implied there. The power law is invariant to the size of the largest fish group present, and so remains constant if an area contains a very large shoal or only much smaller scattered groups of fish, as shown in Fig. 1C. Our observations that very large shoals are structurally similar to much smaller fish groups

must be a consequence of the power law. Knowledge of this power law now enables more accurate statistical predictions of the instantaneous spatial distribution of fish populations over wide areas.

Simultaneous measurements from both the conventional and the waveguide remote-sensing systems show excellent agreement in fish population density at identical time-space points along the conventional line transect (light blue line in Fig. 2, A to D), but only the waveguide technology senses two-dimensional (2D) horizontal structure and temporal change. Both systems reveal dense populations of fish at time-space points α, β, and γ, and neither system registers fish at δ beyond the shoal's seaward edge. The sharp and extensive 2D horizontal boundary of the shoal seen with the waveguide technology along the shelf edge in Figs. 1A and 2, A to D, is too transitory to be inferred from or practically measured with conventional line-transect methods, even from a series of transects. Nor can the conventional system detect or recognize the network of interconnecting bridges between population centers that waveguide technology has shown to be part of the fundamental structure of shoals. For example, the large but transitory bridge connecting the northern and southern wings of the shoal in Fig. 2, A to D, gives it a classic hourglass pattern, never previously observed over such a large scale. This is

[1]Center for Ocean Science and Engineering, Department of Mechanical Engineering, Massachusetts Institute of Technology, 77 Massachusetts Avenue, Cambridge, MA 02139, USA. [2]Department of Electrical and Computer Engineering, Northeastern University, 409 Dana Research Center, Boston, MA 02115, USA. [3]Naval Research Laboratory, Stennis Space Center, MS 39529–5004, USA.

*To whom correspondence should be addressed. E-mail: makris@mit.edu

Fig. 2. A comparison of OAWRS with conventional fish-finding sonar (CFFS). (**A** to **D**) A sequence of instantaneous OAWRS areal density (fish/m²) images taken roughly 10 min apart, starting at 11:59:05 EDT on 14 May 2003, is shown. The color bar is the same as in Fig. 1. The corresponding CFFS transect is overlain in light blue, with the CFFS position for the given OAWRS image indicated by a circle. The white dashed line is the 100-m depth contour. (**E**) Range-depth profile of fish volumetric density (fish/m³) measured by CFFS along the transect shown in (A) to (D). White bars (in the lower black region below the sea floor) correspond to typical time-space points α, β, and γ, where both systems co-register dense fish groups [(A) to (C)]; the gray bar corresponds to point δ in (D), where neither system registers dense fish groups.

missed by the conventional line-transect method (Fig. 2E), which provides no evidence that fish in the γ group are actually well connected to those previously imaged in the β group or occasionally in the α group as well.

We noticed a daily pattern in shoal behavior that involved considerable horizontal migration and thus differed substantially from the day-to-night vertical migrations previously observed with downward-directed sonar in line transects (23, 24). The pattern, observed consistently in the 3 days during which we could monitor large shoals over all daylight hours, began with the horizontal consolidation of shoals in the morning, typically organized by a sharp seaward edge extending for kilometers along a bathymetric contour of the continental shelf edge. Rapid fragmentation and dispersal followed by mid-afternoon, well before sunset when vertical migration began, as shown in Fig. 3, A to D, between 14:20 and 15:00 eastern daylight time (EDT). Fragmentation predictably began with faulting at the bridges between population centers. The bridges were apparently not sufficiently strong to withstand the internal or external pressures to diverge

that acted on the shoal's internal population centers.

To describe this behavior quantitatively, time series of changing fish population (Fig. 3E) were computed at very high sample rates (50-s intervals) from imagery acquired with the waveguide technology over the hundreds of square kilometers immediately encompassing the shoal. We find that total fish population (gray curve of Fig. 3E) decomposes into the sum of a temporally stable (brown curve of Fig. 3E) and a temporally unstable (blue curve of Fig. 3E) time series. The same areal fish density (v_A) threshold (0.2 fish/m²) that separates the temporally stable from the unstable population is also extremely effective in spatially segmenting large shoals from smaller background groups in our instantaneous wide-area images (Figs. 1; 2, A to D; and 3, A to D). The stable component comprises the widely scattered fish groups that would form the observable background scene in the absence of a large shoal. The temporally unstable component effectively characterizes the dramatically dynamic spatial-temporal fluctuations of the large shoal. We believe that fluctuations in total population are pri-

marily due to convergences and divergences in v_A values above and below another threshold [minimum detectable fish density (v_0) = 0.01 fish/m²] where seafloor scattering mechanisms begin to become important and mask fish imaging (15–19). They may also arise from fish groups entering and leaving the survey box.

Time series enable us to introduce the concept of an autocorrelation (25) time scale to quantitatively characterize major temporal fluctuations in shoal population. We find that the autocorrelation time scale ranges between 5 and 10 min (fig. S1A) for the very large shoal of Figs. 1A, 2, and 3, which extends for tens of square kilometers (Fig. 3F). Shoal population (blue curve in Fig. 3E) can fluctuate dramatically in these short time scales, by 20% or a few million fish. Although dramatic, the fluctuations are consistent with the roughly 1 m/s speed at which fish in a shoal typically swim (26–28), as seen from the corresponding areal changes in Fig. 3F. The frequency spectrum of shoal population (fig. S1B) shows no remarkable periodicity, but like the spatial spectrum follows a consistent power-law process that now enables quantitative statistical predictions of

Fig. 3. Evolution of a fish shoal from morning to evening from OAWRS imagery and a time series on 14 May 2003. (**A** to **D**) Four instantaneous OAWRS images or snapshots illustrating morning consolidation and afternoon fragmentation of the shoal. The color bar is the same as in Fig. 1. Vertical arrows indicate snapshot times. (**E**) A time series of population within the area shown in (A) to (D) for v_A within each of the thresholds specified. Gaps in the time series are due to towed-array turns. (**F**) Area occupied by a consolidated shoal or its two largest fragments for $v_A > v_{shoal} = 0.2$ fish/m². (**G**) The internal coherence area is the area within $1/e$ of the 2D autocorrelation peak of instantaneous OAWRS fish density within the shoal or fragment. The centroids of two particular population centers within the shoal are indicated by the circle and the triangle in (A) to (D). (**H**) Relative speeds between the centroids of the two population centers shown in (A) to (D), with mean (blue circle) and standard deviation (bars) shown for each track.
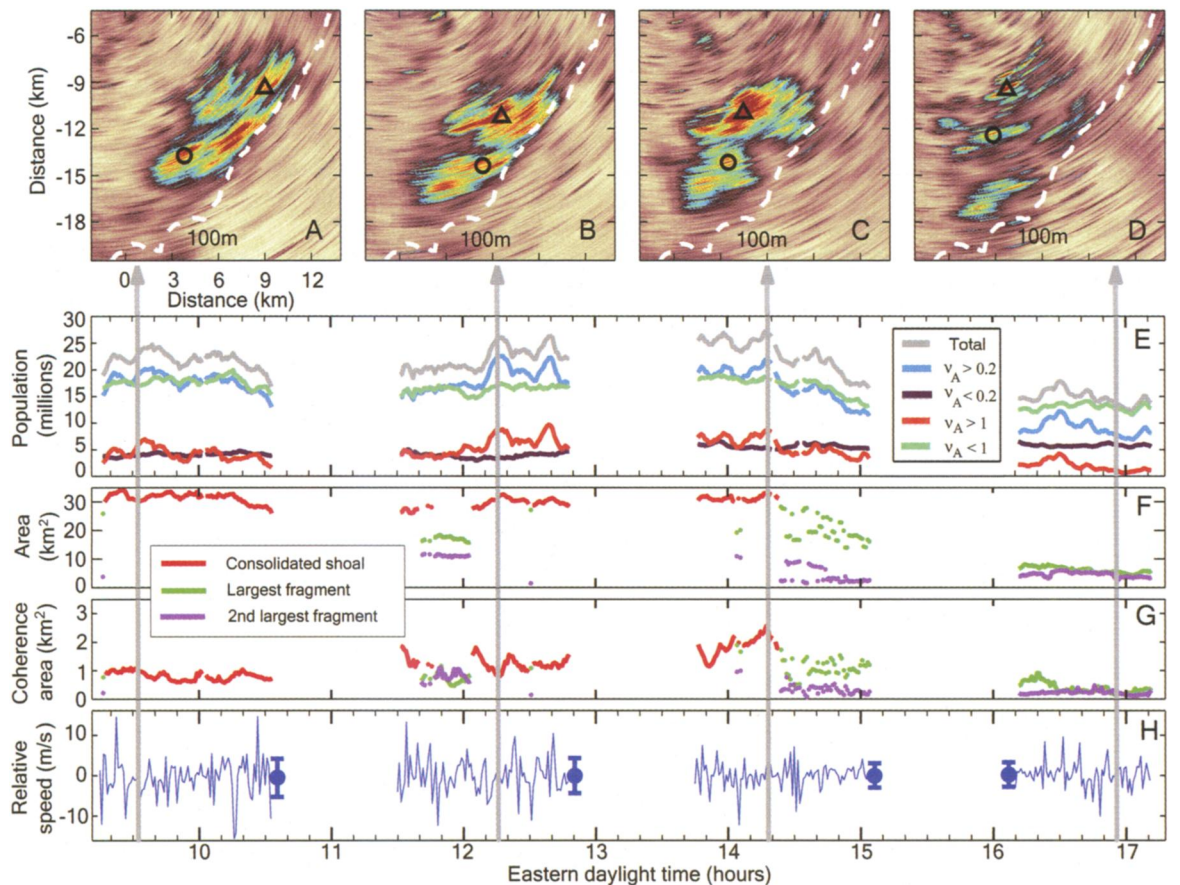
temporal behavior over wide areas and short time scales.

Shoal fragmentation and dispersal also occur very rapidly, as shown in Fig. 3E, where total population plummets in a 30-min period beginning at 14:20 EDT. More than 10 million fish disperse to below the v_0 threshold or leave the survey box. The remaining shoal fragments contain less than half the original shoal population. This and other remotely observed depopulation events were episodic, with peak dispersal rates reaching up to 0.5 million fish/min. Indeed, very large fish shoals were often lost from the view of our conventional line-transect survey system but not from the simultaneous view of our remote-sensing system based on waveguide technology.

Structural similarity can be reexamined in a time-space context by comparing time series of a shoal's outer area (Fig. 3F) to its characteristic internal area of coherence (Fig. 3G), which is the area within which population density is relatively constant. The ratio of these gives an estimate of the number of "degrees of freedom": the independent coherence cells (25) or primary population centers within the shoal or within its largest fragment. The fact that this ratio remains relatively constant over time even after the shoal undergoes severe fragmentation and dispersal is further evidence of structural similarity at all spatial scales, even during such dramatic events, which is consistent with fish assembly and re-assembly models (29). Fluctuations in the shoal's outer area tend to span only a small percentage of the total area. This is true for the inner area only during periods when the shoal is not undergoing fragmentation, as can be seen in Fig. 3, F and G. Otherwise, the inner area fluctuates rapidly, reflecting an internal turbulence that probably fragments shoals.

It is remarkable that both the total population and the internal coherence area attain maxima just before the final fragmentation and dispersal of the shoal. This coincides with the shoal's transformation into a classic hourglass pattern (Fig. 3C). In hourglass patterns, migration from one wing to the other has often been observed when the depopulating wing is under attack by predators (7). Although we have no evidence of such an attack on the shoal in Figs. 2 and 3, and other explanations such as feeding are possible, we do see a massing of population in the northern wing of the hourglass, with a decline of population in the southern wing. This is evident in Fig. 3C and in the subsequent time series of Fig. 3F, where the largest fragment is the northern one and the second largest is the southern one.

The waveguide technology has also revealed the internal motion and migration patterns within very large fish shoals, during time spans ranging from less than 1 min to days, as shown in the imagery sequence of Fig. 2, A to D. Fundamental questions that depend on knowing "the degree of coordination in the movements" between fish populations that were previously "nearly impossible to detect" (6) can now be addressed. We show that even when very large shoals are highly consolidated, densely packed, and structurally similar to small groups of fish, they do not exhibit synchronized motion over short time scales, as much smaller groups often do (10). The many interconnected population centers within a very large shoal have centroids that undergo local positional oscillations in the horizontal, over time scales on the order of minutes, which have no correlation with each other. This is illustrated by the image sequence of Fig. 2, A to D, where velocity vectors for two centroids within the very large shoal are effectively uncorrelated in time and space.

Part of this uncorrelated internal motion arises from fish density waves occurring regularly, every few minutes, as seen by the peak events in Fig. 3H. We identify these as waves because they exceed, by an order of magnitude, the typical speed at which fish swim (26–28). Such waves travel with the apparent speed of an organized sequence of locally interconnected compaction events, like the waves that people propagate in sports stadiums by standing up and sitting down in phase, rather than at the speed at which any individual moves. The waves cause relative displacements of local population centers that are bounded by the roughly 1- to 3-km internal coherence area of Fig. 3G, as can be seen by integrating the separation rate of Fig. 3H over time. Waves have been previously seen in fish shoals spanning scales up to only tens of meters, where they have been hypothesized to provide a rapid means of communication in response to predation or other pressures (10, 30, 31). The most frequent relative motions between the local population centroids, however, occur at the much lower speeds at which individual fish can swim (fig. S1C).

Fish density waves may be used to maintain organizational coherence in very large shoals. The speed, duration, inter-arrival times, and displacements associated with the peak events in Fig. 3H suggest that waves are continuously reflecting from the boundaries of the local population center where they are confined. The waves may then provide a means for individual fish to sense the spatial extent and maintain the coherence of this local subgroup. So far, however, no evidence has appeared of communication over greater distances at a rate faster than fish can swim. Instead, we have observed substantial interaction within shoals spanning tens of kilometers by both bumping and merging of population centers, as well as by population flow across bridges. The relative slowness of this means of communication may be responsible for the inability of shoals to stay together under intense external or internal stresses.

References and Notes

1. R. A. Myers, B. Worm, *Nature* **423**, 280 (2003).
2. J. B. C. Jackson et al., *Science* **293**, 629 (2001).
3. O. Sund, *Nature* **135**, 953 (1935).
4. R. Balls, *J. Cons. Perm. Int. Explor. Mer* **15**, 193 (1948).
5. D. N. MacLennan, E. J. Simmonds, *Fisheries Acoustics* (Chapman and Hall, London, ed. 2, 1992).
6. O. A. Misund, *Fish Biol. Fish.* **7**, 1 (1997).
7. H. Medwin, C. Clay, *Fundamentals of Acoustical Oceanography* (Academic Press, Boston, 1998).
8. F. Gerlotto, M. Soria, P. Fréon, *Can. J. Fish. Aquat. Sci.* **58**, 6 (1999).
9. P. Fréon, O. A. Misund, *Dynamics of Pelagic Fish Distribution and Behavior: Effects on Fisheries and Stock Assessment* (Fishing News Books, Oxford, 1999).
10. T. J. Pitcher, J. Parrish, in *The Behavior of Teleost Fishes*, T. J. Pitcher, Ed. (Chapman and Hall, London, 1993), pp. 363–439.
11. S. Mackinson, U. R. Sumaila, T. J. Pitcher, *Fish. Res.* **31**, 11 (1997).
12. D. P. Croft, J. Krause, I. D. Couzin, T. J. Pitcher, *Fish Fish.* **4**, 138 (2003).
13. W. Siebert, *Circuits, Signals, and Systems* (MIT Press, Cambridge, MA, 1986).
14. Materials and methods are available as supporting material on *Science* Online.
15. N. C. Makris, L. Avelino, R. Menis, *J. Acoust. Soc. Am.* **97**, 3547 (1995).
16. P. Ratilal et al., *J. Acoust. Soc. Am.* **117**, 1977 (2005).
17. N. C. Makris, *J. Acoust. Soc. Am.* **100**, 769 (1996).
18. N. C. Makris, P. Ratilal, *J. Acoust. Soc. Am.* **109**, 909 (2001).
19. P. Ratilal, thesis, Massachusetts Institute of Technology, Cambridge, MA (2002).
20. G. A. Rose, *Nature* **366**, 458 (1993).
21. W. C. Leggett, *Annu. Rev. Ecol. Syst.* **8**, 285 (1977).
22. See www.nmfs.noaa.gov for Spring Bottom Trawl Survey.
23. V. C. Anderson, *J. Acoust. Soc. Am.* **41**, 6 (1967).
24. E. G. Barham, *Science* **151**, 1399 (1966).
25. J. W. Goodman, *Statistical Optics* (Wiley, New York, 1985).
26. I. Huse, E. Ona, *Int. Council Explor. Sea J. Mar. Sci.* **53**, 863 (1996).
27. O. A. Misund, A. Fernö, T. Pitcher, B. Totland, *Int. Council Explor. Sea J. Mar. Sci.* **55**, 58 (1998).
28. D. M. Farmer, M. V. Trevorrow, *J. Acoust. Soc. Am.* **106**, 2481 (1999).
29. T. J. Pitcher, in *Developing and Sustaining World Fisheries Resources: The State of Science and Management, Proceedings of the 2nd World Fisheries Congress*, D. A. Hancock, D. C. Smith, A. Grant, J. P. Beumer, Eds. (Commonwealth Scientific and Industrial Research Organization Publishing, Collingwood, Victoria, Australia, 1997), pp. 143–148.
30. E. Shaw, in *Development and Evolution of Behavior*, L. R. Aronson, E. Tobach, D. S. Lehrman, J. S. Rosenblatt, Eds. (Freeman, San Francisco, CA, 1970), pp. 452–480.
31. G. W. Potts, *J. Zool. London* **161**, 223 (1970).
32. This research was supported by the Office of Naval Research, the Alfred P. Sloan Foundation, and the National Oceanographic Partnership Program, and is a contribution to the Census of Marine Life.